Syntheses, Reactivity, and Molecular Structures of *RSRS*-[Ni(tmc)SC_6H_5](PF_6), *RRSS*-[Ni(tmc)SC_6H_5](CF_3SO_3), and *RRSS*-[Ni(tmc)](CF_3SO_3) (tmc = 1,4,8,11-Tetramethyl-1,4,8,11-tetraazacyclotetradecane)

M. S. Ram,[†] Charles G. Riordan,*[,†] Robert Ostrander,[‡] and Arnold L. Rheingold[‡]

Departments of Chemistry, Kansas State University, Manhattan, Kansas 66506, and University of Delaware, Newark, Delaware 19716

Received June 7, 1995[⊗]

The *RSRS* and *RRSS* isomers of [Ni(tmc)]$(OTf)_2$ (tmc = 1,4,8,11-tetramethyl-1,4,8,11-tetraazacyclotetradecane; $OTf^- = CF_3SO_3^-$) react with $NaSC_6H_5$ to yield the corresponding high spin, five-coordinate derivatives, [Ni(tmc)SC_6H_5](OTf). The molecular structure of each has been determined by X-ray diffraction. *RRSS*-[Ni(tmc)SC_6H_5](OTf) crystallized in the monoclinic space group $P2_1/n$, with a = 12.648(3) Å, b = 15.145(4) Å, c = 14.765(4) Å, β = 113.96(2)°, V = 2584(1) Å^3, and Z = 4. The coordination sphere about Ni is best described as square pyramidal with a Ni−S bond distance of 2.369(2) Å and Ni−N_{av} of 2.128Å. *RSRS*-[Ni(tmc)SC_6H_5](PF_6) crystallized in the monoclinic space group $P2_1/n$, with a = 13.037(5) Å, b = 15.407(7) Å, c = 13.706(7) Å, β = 113.53(3)°, V = 2524(2) Å^3, and Z = 4. The Ni resides in a highly distorted square pyramid with a shorter Ni−S distance, 2.352(2)Å and correspondingly longer Ni−N_{av} distance of 2.149Å. Alternatively [Ni(tmc)SR](OTf) may be produced by oxidative addition of disulfide, R_2S_2 (R = C_6H_5, C_2H_5), to Ni(tmc)(OTf). The second-order rate constant, k_1, for reaction with $(C_6H_5)_2S_2$ is 120 $M^{-1}s^{-1}$. $(C_2H_5)_2S_2$ reacts 5 orders of magnitude more slowly consistent with its greater S−S bond dissociation energy. The nickel thiolates react with haloalkanes, RX (RX = CH_3I, C_2H_5I, $(CH_3)_2CHI$, $C_6H_5CH_2Cl$), producing [Ni(tmc)X](OTf) and C_6H_5SR. The reaction is second order with k_2 decreasing in the order, CH_3I > C_2H_5I > $(CH_3)_2CHI$. Strikingly, for reactions with a given RX, the *RRSS* isomer reacted *ca.* 350 times faster than the *RSRS* isomer. *RRSS*-[Ni(tmc)](OTf)·Na(OTf) has also been characterized, having crystallized in the monoclinic space group $C2/c$, with a = 24.690(13) Å, b = 11.261(5) Å, c = 9.681(6) Å, β = 91.03(4)°, V = 2691(2) Å^3, and Z = 4. The macrocycle provides the Ni(I) ion with a square planar coordination environment in which there are two distinct Ni−N bond distances, 2.120(5) and 2.095(5) Å.

Introduction

F_{430} is the nickel-containing prosthetic group of methyl coenzyme M reductase which, in the final step of methanogenesis, catalyzes the reductive cleavage of methyl coenzyme M (MeCoM)[1] in the presence of a thiol cofactor to produce methane and a mixed disulfide, eq 1.[2] The enzyme also appears

$$CH_3{-}SCH_2CH_2SO_3^- + HS{-}HTP \xrightarrow{\text{MeCoM reductase}} CH_4 + {}^-O_3SCH_2CH_2S{-}S{-}HTP \quad (1)$$

to be involved in the reductive dehalogenation of chlorinated hydrocarbons by methanogenic bacteria.[3] The structure of F_{430} has been established (Chart 1) and the nickel appears to be redox active cycling between Ni(II) and Ni(I) during catalysis.[4] While the specific mechanism by which the enzyme catalyzes C−S bond rupture remains unclear, the Ni(I) state of *isolated* F_{430} does not react directly with organosulfides including MeCoM.[5]

Chart 1

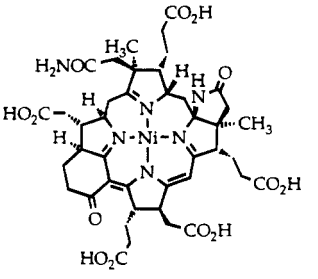

F_{430}

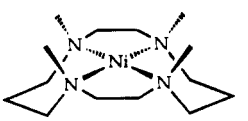

RSRS-Ni(tmc)$^{2+}$

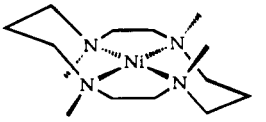

RRSS-Ni(tmc)$^{2+}$

* To whom correspondence should be addressed. E-mail: Riordan@ksu.ksu.edu.
[†] Kansas State University.
[‡] University of Delaware.
[⊗] Abstract published in *Advance ACS Abstracts,* October 15, 1995.

(1) Abbreviations: MeCoM, $CH_3SCH_2CH_2SO_3^-$; HS−HTP, (7-mercaptoheptanoyl)threonine phosphate; dioxo[16]aneN$_5$, 1,4,7,10,13-pentaazacyclohexadecane-14,16-dione; tmc, 1,4,8,11-tetramethyl-1,4,8,11-tetraazacyclotetradecane; OTf^-, $CF_3SO_3^-$; Me_{10}[14]aneN$_4$, 1,4,5,7,7,8,11,12,14,14-decamethyl-1,4,8,11-tetraazacyclotetradecane; tc1, 8-methyl-1,3,6,8,10,13,15-heptaazatricyclo[13.1.1.1^{13,15}]octadecane; tc2, 1,3,6,9,-11,14-hexaazamacrotricyclo[12.2.1.1^{6,9}]octadecane; htim, 2,3,9,10-tetramethyl-1,4,8,11-tetraazacyclotetradecane; diene, 5,7,7,12,14,14-hexamethyl-1,4,8,11-tetraazacyclotetra-4,11-diene; OEP, 2,3,7,8,12,12,17,18-octaethylporphyrinato dianion; [14]ane-N$_4$, 1,4,8,-11-tetraazacyclotetradecane.

(2) (a) Gunsalus, R. P.; Wolfe, R. S. *FEMS Microbiol. Lett.* **1978**, *3*, 191−193. (b) Ellefson, W. L.; Whitman, W. B.; Wolfe, R. S. *Proc. Natl. Acad. Sci. U.S.A.* **1982**, *79*, 3707−3710. (c) Pfaltz, A.; Livingston, D. A.; Juan, B.; Diekert, G.; Thauer, R.K.; Eschenmoser, A. *Helv. Chim. Acta* **1985**, *68*, 1338−1358. (d) Kovacs, J. A. *Advances in Inorganic Biochemistry*; Eichorn, G. L.; Marzilli, L. G., Eds.; Prentice-Hall: Englewood Cliffs, NJ, 1993; Vol. 9, Chapter 5. (e) Halcrow, M. A.; Christou, G. *Chem. Rev.* **1994**, *94*, 2421−2481.

0020-1669/95/1334-5884$09.00/0

$Ni(I)-F_{430}$ does react with CH_3I to produce methane via a $Ni-CH_3$ intermediate.[5] While these results have motivated model studies aimed at elucidating mechanistic parameters for the activation of MeCoM,[6] only one system, Ni(dioxo[16]aneN_5),[6a] liberates stoichiometric quantities of methane from MeCoM. However, the oxidative nature of this system seems incompatible with our current knowledge of F_{430}.

To further our understanding of the F_{430}-catalyzed system, we have examined reactions of organosulfides, thiols and disulfides with $[Ni(tmc)](OTf)_2$ and [Ni(tmc)](OTf). $[Ni(tmc)](OTf)_2$ exists predominantly as two isomers, *RSRS* and *RRSS* (Chart 1).[7] These may be prepared by alternate synthetic routes and they do not equilibrate in solution at room temperature.[8] The tmc ligand was chosen as a model for F_{430} based on the following criteria. (1) As the Ni(II)/Ni(I) redox couple appears to be involved in the catalytic reduction of MeCoM by F_{430}, we sought a N_4 macrocycle which would stabilize these oxidation states to a similar extent as F_{430}. The redox couples for $Ni(tmc)^{2+/+}$, $E_{1/2} = -0.780$ V (CH_3CN, vs Ag/AgCl) for the *RSRS* isomer and −0.960 V for the *RRSS* isomer,[9] are very close to the redox couple for F_{430M} (the pentamethylester of F_{430}), $E_{1/2} = -0.748$ V.[10] Therefore, the reducing potential of [Ni(tmc)](OTf) mirrors that of F_{430M}. (2) Several researchers have invoked a $Ni-CH_3$ intermediate during methyl coenzyme M reductase catalysis.[2d,e] Perhaps consistent with this proposal low temperature alkylation of $Ni(I)-F_{430M}$ with CH_3I or $(CH_3)_3S^+$ results in formation of a $Ni-CH_3$ intermediate.[5] Subsequent hydrolysis of the $Ni-CH_3$ bond produces methane. [Ni(tmc)](OTf) may also be alkylated to yield an isolable $Ni-CH_3$ species.[9b,11] (3) The tmc ligand is sufficiently flexible to permit binding of exogenous ligands in axial coordination sites. In acetonitrile, *RSRS*-$[Ni(tmc)](OTf)_2$ exists as a five-coordinate, square pyramidal complex solvated with one CH_3CN.[12] *RRSS*-$[Ni(tmc)](OTf)_2$ binds two CH_3CN to form a six-coordinate species. Notably, both F_{430M} and $[Ni(tmc)](OTf)_2$ bind imidazole strongly, the former yielding a six-coordinate adduct.[13]

Herein we report the syntheses, characterization and reactivity patterns of *RSRS*-$[Ni(tmc)SC_6H_5](OTf)$ and *RRSS*-$[Ni(tmc)SC_6H_5](OTf)$, accessible by several synthetic routes, including oxidative addition of $(C_6H_5)_2S_2$ to [Ni(tmc)](OTf). This represents the first structural account of five-coordinate complexes of both the *RSRS* and *RRSS* isomers. As such it permits comparison of relevant metric parameters. Solid state structural differences are reflected in the rates of alkylation of $[Ni(tmc)SC_6H_5](OTf)$ with haloalkanes. During the course of this study, we have crystallographically characterized *RRSS*-[Ni(tmc)](OTf), a structural model for the reduced form of F_{430}.

Experimental Section

Materials and Methods. All reagents were distilled under N_2 and dried as indicated. THF, Et_2O, and benzene were freshly distilled over Na/benzophenone. Acetonitrile was distilled over CaH_2 and collected after discarding the first fraction. Haloalkanes were distilled over CaH_2 at reduced pressures under N_2 and were stored protected from light over Cu wire. $(C_2H_5)_2S_2$ was distilled under reduced pressure. $(C_6H_5)_2S_2$ was used as received. Elemental analyses were performed by Desert Analytics and Schwarzkopf Microanalytical, Inc. Electronic spectra were recorded with a SLM-Aminco 3000 diode array spectrophotometer. NMR spectra were recorded on a 400 MHz Brüker spectrometer equipped with a Sun workstation. GC-MS were performed on a Hewlett-Packard 5989A mass spectrometer equipped with a HP 5890-II gas chromatograph. Kinetic experiments were monitored by UV−visible spectroscopy in cuvettes which were temperature regulated in a thermostated cell holder equilibrated with a circulating bath. Cyclic voltammetry was performed on a BAS 50W voltammetric analyzer. Experiments were performed in an Ar-filled glovebox in a cell consisting of a glassy carbon working electrode (1 mm), Pt wire counter electrode and Ag/AgCl reference electrode. Solutions contained 0.1 M electrolyte ($[Bu_4N][PF_6]$) and 2−5 mM sample. Potentials were referenced to internal Fc/Fc^+ (+410 mV vs Ag/AgCl). *RRSS* and *RSRS*-$[Ni(tmc)](OTf)_2$ were prepared according to Barefield.[14] The corresponding PF_6^- salts were obtained from the triflates by precipitation from water upon addition of aqueous $[NH_4][PF_6]$. The isomeric purity of the nickel(II) complexes was determined by their aqueous electronic spectra, λ_{max}, nm (ϵ, M^{-1} cm^{-1}): *RSRS*, 395 (103), 514 (66), 654 (30); *RRSS*, 494 (27), 367 (10). In general, the *RRSS* derivatives were found to be less soluble than the *RSRS* species. $NaSC_6H_5$ was prepared by addition of C_6H_5SH (2.0 g, 18 mmol) to Na metal (600 mg, 26 mmol) in 30 mL THF. $NaSC_6H_5$ precipitated as a white powder, was dried under reduced pressure at 60 °C for 12 h and stored in the glovebox. The salt was extremely hygroscopic.

$[Bu_4N][MeCoM]$. [Na][MeCoM] was prepared according to Wolfe.[15] The Bu_4N^+ salt could not be prepared by simple solution metathesis with $[Bu_4N]Cl$. The cation exchange resin Sephadex SP-C-25 was converted to the acid by treatment with CF_3SO_3H. The acid form of the exchange resin was treated with $[Bu_4N]OH$ and washed with water several times to obtain the Bu_4N^+ exchange resin. An aqueous solution of [Na][MeCoM] was passed through the exchange resin and the resulting solution was rotary evaporated to dryness. $[Bu_4N][MeCoM]$: ^1H NMR (D_2O) δ 3.27 (t, CH_2SO_3, 2 H), 3.23 (m, NCH_2, 8 H), 2.95 (t, SCH_2, 2H), 2.21 (s, SCH_3, 3 H), 1.70 (m, CH_2, 8 H), 1.40 (m, CH_2, 8 H), 1.00 (t, CH_3, 12 H). Although $[Bu_4N][MeCoM]$ was soluble in organic solvents, it precipitated in the presence of [Ni(tmc)](OTf) even in Me_2SO. $[Bu_4N][MeCoM]$ did not precipitate upon addition of $[Ni(tmc)](OTf)_2$.

***RRSS*-[Ni(tmc)](OTf)·Na(OTf).** $[Ni(tmc)](OTf)_2$ (either isomer) (1.0 g, 1.6 mmol) was stirred with 50 g of Na/Hg (0.3%) in 22 mL of

(3) (a) Krone, U. E.; Laufer, K.; Thauer, R. K.; Hogenkamp, H. P. C. *Biochemistry* **1989**, *28*, 10061−10065. (b) Fathepure, B. Z.; Boyd, S. A.; *FEMS Microbiol. Lett.* **1988**, *49*, 149−165.

(4) (a) Albracht, S. P. J.; Ankel-Fuchs, D.; Böcher, R.; Ellermann, J.; Moll, J.; van der Zwaan, J. W.; Thauer, R. K. *Biochem. Biophys. Acta* **1988**, *955*, 86−102. (b) Albracht, S. P. J.; Ankel-Fuchs, D.; van der Zwaan, J. W.; Fontjin, R. D.; Thauer, R. K. *Biochem. Biophys. Acta* **1986**, *870*, 50−57.

(5) (a) Juan, B.; Pfaltz, A. *J. Chem. Soc., Chem. Commun.* **1988**, 293−94. (b) Lin, S. K.; Juan, B. *Helv. Chim. Acta* **1991**, *74*, 1725−1738.

(6) (a) Drain, C. M.; Sable, D. B.; Corden, B. B. *Inorg. Chem.* **1988**, *27*, 2396−2398. (b) Drain, C. M.; Sable, D. B.; Corden, B. B. *Inorg. Chem.* **1990**, *29*, 1428−1433. (c) Stolzenberg, A. M.; Stershic, M. T. *J. Am. Chem. Soc.* **1988**, *110*, 5397−5403. (d) Lahiri, G. K.; Schussel, L. J.; Stolzenberg, A. M. *Inorg. Chem.* **1992**, *31*, 4991−5000. (e) Lahiri, G. K.; Stolzenberg, A. M. *Inorg. Chem.* **1993**, *32*, 4409−4413. (f) Helvenston, M. C.; Castro, C. E. *J. Am. Chem. Soc.* **1992**, *114*, 8490−8496. (g) Cha, M.; Shoner, S. C.; Kovacs, J. A. *Inorg. Chem.* **1993**, *32*, 1860−1863. (h) Zilbermann, I.; Golub, G.; Cohen, H.; Meyerstein, D. *Inorg. Chim. Acta* **1994**, *227*, 1−3.

(7) The Cahn−Prelog−Ingold designation of the nitrogen configurations indicates their chirality. The two isomers of present interest, *RSRS* and *RRSS*, correspond to the *Trans I* and *Trans III* designations, respectively, proposed by Bosnich. Bosnich, B.; Poon, C. K.; Tobe, M. I. *Inorg. Chem.* **1965**, *4*, 1102−1108.

(8) Equilibration does occur in Me_2SO at elevated temperatures. Moore, P.; Sachinidis, J.; Willey, G. R. *J. Chem. Soc., Chem. Commun.* **1983**, 522−523.

(9) (a) Barefield, E. K.; Freeman, G. M.; Van Derveer, D. G. *Inorg. Chem.* **1986**, *25*, 552−558. (b) Ram, M. S.; Riordan, C. G. *J. Am. Chem. Soc.* **1995**, *117*, 2365−2366.

(10) Juan, B.; Pfaltz, A. *J. Chem. Soc., Chem. Commun.* **1986**, 1327−1329.

(11) (a) Bakac, A.; Espenson, J. H. *J. Am. Chem. Soc.* **1986**, *108*, 713−719. (b) Ram, M. S.; Bakac, A.; Espenson, J. H. *Inorg. Chem.* **1986**, *25*, 3267−3272 . Alternatively, $Ni(tmc)CH_3^+$ may be prepared by methathesis: D'Aniello, M. J.; Barefield, E. K. *J. Am. Chem. Soc.* **1976**, *98*, 1610−1611.

(12) (a) Herron, N.; Moore, P. *Inorg. Chim. Acta* **1979**, *36*, 89−96. (b) Moore, P.; Sachinidis, J.; Willey, G. R. *J. Chem. Soc. Dalton Trans.* **1984**, 1323−1327.

(13) Fässler, A. Dissertation, ETH, Zürich, No. 7799, 1985.

(14) (a) Wagner, F.; Barefield, E. K. *Inorg. Chem.* **1973**, *12*, 2435−2439. (b) Wagner, F; Barefield, E. K. *Inorg. Chem.* **1976**, *15*, 408−417.

(15) Gunsalus, R. P.; Romesser, J. A.; Wolfe, R. S. *Biochemistry* **1978**, *17*, 2374−2377.

THF−CH_3CN (10:1). After 30 min, the solution was filtered and the product precipitated by addition of Et_2O and hexanes. Recrystallization from THF−Et_2O yielded blue-green crystals of [Ni(tmc)](OTf) cocrystallized with NaOTf in greater than 90% yield. Electronic spectrum (THF): λ_{max}, nm (ϵ, M^{-1} cm^{-1}) 351 nm (4000). Anal. Calcd for $C_{16}H_{32}F_6N_4NaNiO_6S_2$: C, 30.20; H, 5.03; N, 8.89. Found: C, 30.04; H, 4.99; N, 8.51. [Ni(tmc)](OTf) was extremely O_2 sensitive, turning readily to red upon exposure to air.

***RSRS*-[Ni(tmc)SC_6H_5](PF_6).** Addition of $NaSC_6H_5$ (35 mg, 0.27 mmol) to a THF slurry of *RSRS*-[Ni(tmc)](PF_6)$_2$ (170 mg, 0.28 mmol) resulted in an immediate change from a purple suspension to a deep orange solution. After 5 min, the solution was filtered and the product precipitated by addition of Et_2O and hexanes. Isolated yield: 120 mg (80%). Electronic spectrum (THF), λ_{max}, nm (ϵ, M^{-1} cm^{-1}): 475 nm (3000), 341 nm (2330). Anal. Calcd for $C_{20}H_{37}F_6N_4NiPS$: C, 42.17; H, 6.50; N, 9.84. Found: C, 42.41; H, 6.52; N, 9.71. In solution, this isomer lost tmc readily in the presence of trace moisture. X-ray quality crystals were grown by diffusing Et_2O into a concentrated THF−hexanes (90:10) solution.

***RRSS*-[Ni(tmc)SC_6H_5](PF_6).** This complex was prepared similarly to the *RSRS* isomer, except THF−CH_3CN (4:1) replaced neat THF as solvent, owing to the poorer solubility of this isomer in THF. Isolated yield: 90 mg (60%). Electronic spectrum (THF), λ_{max}, nm (ϵ, M^{-1} cm^{-1}): 469 nm (3000), 362 nm (2220). Anal. Calcd for $C_{20}H_{37}F_6N_4NiPS$: C, 42.17; H, 6.50; N, 9.84. Found: C, 42.25; H, 6.38; N, 10.02. The more soluble triflate salts of both *RSRS*- and *RRSS*-[Ni(tmc)SC_6H_5]$^+$ were prepared in an analogous manner and had identical electronic spectral features. X-ray quality crystals of the OTf^- salt were grown by slowly cooling a concentrated THF−hexanes (90:10) solution to −35 °C.

Spectral Titrations. Titrations were performed in acetone because the *RRSS*- and *RSRS*-[Ni(tmc)](OTf)$_2$ complexes are four coordinate in this solvent as indicated by the presence of only the 514 nm band in the visible spectra. Addition of potential ligands Me_2SO, CH_3CN, $RSCH_3$ (R = CH_3, C_2H_5), $NaSC_6H_5$, to *RSRS*-[Ni(tmc)](OTf)$_2$ (15 mM) resulted in diminution of the 514 nm feature with concomitant appearance of two new bands at 394 nm and 650 nm. Titrations were continued until addition of subsequent aliquots of ligand produced no further spectral changes. The number of exogenous ligands bound (slopes) and binding constants (y-intercepts) were determined from linear plots of ln[($A - A_0/A_\infty - A$)] vs ln [ligand]. In cases where the binding was strong, K was estimated relative to that of CH_3CN as exemplified by $SC_6H_5^-$ ligation. For $SC_6H_5^-$ binding in CH_3CN, $K^{SC_6H_5}[SC_6H_5^-]/K_1[CH_3CN] = [Ni(tmc)SC_6H_5(OTf)]/[Ni(tmc)(NCCH_3)(OTf)_2]$. At [Ni(tmc)$SC_6H_5$(OTf)] = 2 mM ([$CH_3CN$] = 20 M), binding was complete as measured by UV−visible spectroscopy ([Ni(tmc)SC_6H_5(OTf)]/[Ni(tmc)(NCCH$_3$)(OTf)$_2$] > 10), which sets a lower limit on $K^{SC_6H_5}$ of 10^5 M^{-1}. Similar analysis with I^- competing with $SC_6H_5^-$ yielded $K^{SC_6H_5} > 10^6$ M^{-1}.

Cyclic Voltammetric Measurements. The equilibrium binding constant for $SC_6H_5^-$, $K^{SC_6H_5}$, was measured independently by an electrochemical method. In the presence of 1 equiv of $NaSC_6H_5$, the Ni(II/I) redox potential of [Ni(tmc)](OTf)$_2$ shifted to −0.95 V (CH_3CN, vs Ag/AgCl). Since Ni(I) does not bind exogenous ligands, the shift in potential reflects Ni(II) binding $SC_6H_5^-$. Applying the Nerst equation yields a lower limit for $K^{SC_6H_5}$ of 10^6 M^{-1}. Further addition of $NaSC_6H_5$ was not possible due to significant precipitation and decomposition. Therefore, we were left with only a lower limit for the binding constant. However, this value agrees with that measured spectrophotometrically. The cyclic voltammetry method yielded identical $K^{SC_6H_5}$ values for both *RSRS*- and *RRSS*-[Ni(tmc)](OTf)$_2$.

Product Analysis. Production of thioanisole, $C_6H_5SCH_3$, from reactions of *RSRS*- and *RRSS*-[Ni(tmc)SC_6H_5](OTf) with CH_3I was confirmed by GC−MS analysis. In a typical experiment, 2 equiv of CH_3I (20 mM) was added to [Ni(tmc)SC_6H_5](OTf) (10 mM) in THF. After 12 h, 0.5 μL aliquots were injected onto a RTX-5 column. The column temperature was programmed as follows: 70 °C for 1 min and then ramping at 20 °C/min to 200 °C. Thioanisole production was determined by its characteristic retention time, 4.86 min, and mass spectral features, (M^+, *m/e* 124). These data were identical with those of an authentic sample of thioanisole. Yields were greater than 90%.

Kinetics. [Ni(tmc)](OTf) + $(C_2H_5)_2S_2$. THF solutions of [Ni(tmc)](OTf) were prepared in a spectrophotometric cell inside a Ar-filled glovebox. Reactions were initiated by injecting neat Et_2S_2 into thermostated Ni(I) solutions through a septum-capped sidearm. Rates were measured by monitoring absorbance increases at 414 nm (λ_{max} for [Ni(tmc)SC_2H_5](OTf)) or absorbance decreases at 351 nm (λ_{max} for [Ni(tmc)](OTf)). Values of k_{obs} were obtained from the slope of plots of ln($A - A_\infty$) vs time which were linear over 3 half-lives. A plot of k_{obs} vs [$(C_2H_5)_2S_2$] was also linear, confirming the first order dependence on [$(C_2H_5)_2S_2$].

[Ni(tmc)](OTf) + $(C_6H_5)_2S_2$. This reaction was too rapid to monitor by conventional spectrophotometric methods even under high dilution. However, an estimate of k_{obs} was obtained from the second half of the reaction under second order conditions: [[Ni(tmc)](OTf)] = 2 mM, [$(C_6H_5)_2S_2$] = 1 mM, $t_{1/2}$ = 8 s. These data yielded a crude estimate for the second-order rate constant of approximately 120 M^{-1} s^{-1}. A more accurate determination of the rate constant was obtained by cyclic voltammetry.[16] In CH_3CN, with [Bu_4N][PF_6] (0.1 M) as supporting electrolyte, the cyclic voltammograms of [Ni(tmc)](OTf)$_2$ (2.5 mM) were obtained in the presence of 0, 10, 20, 44, and 91 mM $(C_6H_5)_2S_2$. The scan rate for each [$(C_6H_5)_2S_2$] was varied: 50, 100, 200, 500, 1000, and 2000 mV/s. E_f for [Ni(tmc)](OTf)$_2$ was at −0.78 V. The cathodic and anodic currents were measured and corrected for background currents. Thus τ = 220 mV/scan rate, where τ is defined as the time required to scan from the formal potential to the switching potential (−1.0 V) and the scan rate is the estimated scan rate at which $i_a = i_c/2$.[16] The pseudo first order rate constant, k_{obs}, is the inverse of τ under these conditions. A linear plot of k_{obs} vs [$(C_6H_5)_2S_2$] yielded the second-order rate constant of 120 M^{-1} s^{-1}. It should be noted that this method of obtaining rate constants from current ratios provides only an estimate and not a precise rate constant compared to other electrochemical or spectral methods. This approach was applied to *RSRS*-[Ni(tmc)](OTf)$_2$ in CH_3CN but could not be applied to the *RRSS* isomer because its reduction interfered severely with the direct electrochemical reduction of $(C_6H_5)_2S_2$ in CH_3CN.

[Ni(tmc)SC_6H_5](OTf) + RX. Stock solutions of [Ni(tmc)SC_6H_5](OTf) in THF-CH_3CN (1:1)[17] were prepared in a Ar-filled glovebox. Aliquots (0.5−1.0 mM) were transferred to a 1 cm quartz spectrophotometric cell which was sealed under Ar with a Kontes rotoseal tap. Reactions were initiated by injecting the appropriate amount of haloalkane through a septum-capped sidearm. Rates were measured by monitoring absorbance changes at 463 nm (occasionally at 485 nm) corresponding to the disappearance of [Ni(tmc)SC_6H_5](OTf). Values of k_{obs} were obtained from the slope of plots of ln($A - A_\infty$) vs time which were linear over three half-lives. Plots of k_{obs} vs [RX] were also linear, confirming the first order dependence on [RX]. In two cases where the reactions were slowest, $(CH_3)_2CHI$ and $C_6H_5CH_2Cl$ reacting with *RSRS*-[Ni(tmc)SC_6H_5](OTf), there were significant deviations from pseudo-first-order behavior. In these instances, the initial 10% of the data were in accord with pseudo-first-order behavior, while deviations in the latter data were consistent with competitive Ni−SC_6H_5 bond rupture followed by fast alkylation of $SC_6H_5^-$ in solution.

Crystallographic Structural Determinations. Crystallographic data for the structures are collected in Table 1 and in the Supporting Information. Specimens were mounted on glass fibers and found photographically to possess 2/*m* Laue symmetry. Systematic absences in the diffraction allowed unique assignments of space groups. The data sets were semiempirically corrected for absorption and solved by heavy-atom methods. All non-hydrogen atoms were refined anisotropically and hydrogen atoms were idealized. All computations used SHELXTL-PC software (Ver. 4.2, G. Sheldrick. Siemens XRD, Madison, WI).

Results and Discussion

Organic Sulfide Binding to Ni(tmc)(OTf)$_2$. *RSRS*- and *RRSS*-[Ni(tmc)](OTf)$_2$ react cleanly with organic sulfides, RSR′,

(16) Nicholson, R. S.; Shain, I. *Anal. Chem.* **1964**, *36*, 706−723.
(17) This solvent mixture was necessary because (i) *RRSS*-[Ni(tmc)]I_2 precipitated in neat THF, interfering with the spectrophotometric monitoring, and (ii) the kinetics were too rapid to follow in neat CH_3CN.

Table 1. Crystallographic Data

	RRSS-[Ni(tmc)](OTf)·NaOTf	*RRSS*-[Ni(tmc)SC_6H_5](OTf)	*RSRS*-[Ni(tmc)SC_6H_5](PF_6)
formula	$C_{16}H_{32}F_6N_4NaNiO_6S_2$	$C_{21}H_{37}F_3N_4NiO_3S_2$	$C_{20}H_{37}F_6N_4NiPS$
fw	636.3	573.4	569.3
color, habit	blue-green plate	red-orange block	dark orange block
cryst syst	monoclinic	monoclinic	monoclinic
space group	*C2/c*	$P2_1/n$	$P2_1/n$
a, Å	24.690(13)	12.648(3)	13.037(5)
b, Å	11.261(5)	15.145(4)	15.407(7)
c, Å	9.681(6)	14.765(4)	13.706(7)
β, deg	91.03(4)	113.96(2)	113.53(3)
V, Å^3	2691(2)	2584(1)	2524(2)
Z	4	4	4
T, K	296	240	246
λ(Mo Kα), Å	0.710 73	0.710 73	0.710 73
ρ(calcd), g cm^{-3}	1.570	1.474	1.498
μ, cm^{-1}	9.22	9.64	9.75
$R(F)$, $R_w(F)$[a]	0.050, 0.059	0.059, 0.087	0.064, 0.073

[a] $R(F) = \Sigma\Delta/\Sigma(F_o)$; $R_w(F) = \Sigma[\Delta w^{1/2}]/[F_o w^{1/2}]$; $\Delta = |F_o - F_c|$; $w^{-1} = \sigma^2(F_o) + gF_o^2$.

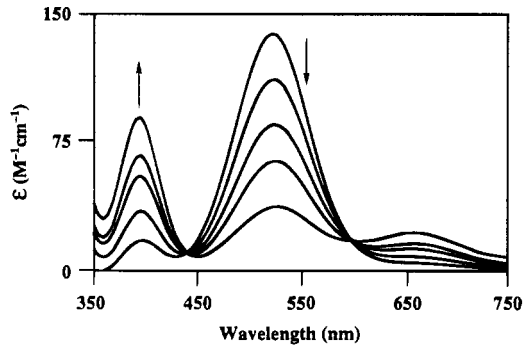

Figure 1. UV−visible spectral titration (acetone) of *RSRS*-[Ni(tmc)](OTf)$_2$ (5.0 mM) with $(CH_3)_2S$ (0, 2.8, 5.5, 6.9, and 9.3 M, respectively) at 25 °C.

Table 2. Equilibrium Binding Constants for *RSRS*-[Ni(tmc)](OTf)$_2$ Measured in Acetone at 25 °C

L	*K*, M^{-1}	L	*K*, M^{-1}
$(CH_3)_2S$	0.10	$SC_6H_5^-$	$>10^6$ [b]
$CH_3SC_2H_5$	0.08	$(CH_3)_2SO$	1.0[a]
$CH_3SC_6H_5$	0	H_2O	0.50[a]
$(C_6H_5)_2S_2$	0	CH_3CN	3.0[a]

[a] Reference 12. [b] Measured in CH_3CN.

in acetone to yield high spin, five-coordinate species. Binding is accompanied by distinct electronic spectral changes. For example, addition of $(CH_3)_2S$ to *RSRS*-[Ni(tmc)](OTf)$_2$ resulted in disappearance of the 523 nm band with concomitant appearance of a band at 395 nm, Figure 1. Isosbestic points occurred at 440 and 600 nm. Binding constants were extracted from spectral titrations, Table 2. These spectroscopic changes are consistent with those reported for [Ni(tmc)](OTf)$_2$ in donor solvents such as H_2O, Me_2SO, and CH_3CN.[12] Under these conditions, *RSRS*-[Ni(tmc)](OTf)$_2$ forms five-coordinate, square pyramidal complexes while *RRSS*-[Ni(tmc)](OTf)$_2$ binds two solvent molecules in axial positions yielding six-coordinate derivatives. Dialkylsulfides bind weakly to [Ni(tmc)](OTf)$_2$. Even with [$(CH_3)_2S$] of 9 M, *RRSS*-[Ni(tmc)](OTf)$_2$ formed the five-coordinate adduct. Binding constants were relatively insensitive (± 10%) to the Ni isomer. Aryl-substituted sulfides, as exemplified by thioanisole, showed no evidence of binding even at 5 M concentrations.

The disulfides $(C_2H_5)_2S_2$ and $(C_6H_5)_2S_2$ showed no evidence of coordinating to either isomer of [Ni(tmc)](OTf)$_2$. The thiolates $SC_6H_5^-$ and $SC_2H_5^-$ bind strongly to [Ni(tmc)](OTf)$_2$ yielding high spin, five-coordinate species in acetonitrile. The equilibrium constant for $SC_6H_5^-$ binding to *RSRS*-[Ni(tmc)](OTf)$_2$, as measured spectrophotometrically and electrochemically in acetonitrile, is *ca.* 10^6 M^{-1}.

MeCoM Binding to *RSRS*-[Ni(tmc)](OTf)$_2$. In contrast to organic sulfides, MeCoM binds avidly to *RSRS*-[Ni(tmc)](OTf)$_2$. Stoichiometric amounts of MeCoM are sufficient to observe complete binding ($K^{MeCoM} > 10^6$ M^{-1}). ^{1}H NMR and IR spectra are consistent with MeCoM binding to Ni through the SO_3^-. In the ^{1}H NMR spectrum (acetone-d_6), the methylene protons of MeCoM resonate at −5.4 ppm ($CH_2SO_3^-$) and −0.6 ppm ($CH_2CH_2SO_3^-$) while the methyl protons occur furthest downfield −0.04 ppm (CH_3S). In the IR spectrum, the ν_{SO} bands are shifted from 1195 cm^{-1} for uncomplexed MeCoM to 1245 cm^{-1}, with a reduction in intensity of more than 50% accompanying binding to *RSRS*-[Ni(tmc)](OTf)$_2$. Binding through the sulfonate is expected based on favorable electrostatic attraction between the 2+ charged Ni ion in *RSRS*-[Ni(tmc)](OTf)$_2$ and the negatively charged SO_3^-. Other anionic ligands, such as N_3^-,[14a] OH^-, and SR^-, exhibit similar high affinities for *RSRS*-[Ni(tmc)](OTf)$_2$. *In vivo*, the sulfonate is most likely involved in H-bonding to residues near the active site of F_{430} which deactivates this group towards binding at Ni and probably directs the thioether of the substrate toward the Ni ion.[2,6b] Additionally, the hydrocorphinoid macrocycle in F_{430} carries a single anionic charge which renders the Ni(I) complex electroneutral and less likely to bind MeCoM through the sulfonate. The former may be significant in understanding the inability of F_{430} to liberate CH_4 from MeCoM *in vitro*. Under these conditions the sulfonate may compete effectively with the thioether for ligation at Ni. By binding to the Ni ion, the sulfonate occupies an open coordination site which is needed for catalysis. Results presented above suggest that for *RSRS*-[Ni(tmc)](OTf)$_2$, $K^{SO_3^-} \geq 10^7 K^{R_2S}$.

Synthesis of [Ni(tmc)](OTf). The cyclic voltammagram of *RSRS*-[Ni(tmc)](OTf)$_2$ in CH_3CN exhibited a single, electrochemically reversible (ΔE = 65 mV) redox couple at −780 mV (vs Ag/AgCl). The *RRSS* isomer is somewhat more difficult to reduce in CH_3CN: $E_{1/2}$ = −960 mV. In acetone, both isomers are reduced at identical potentials, $E_{1/2}$ = −780 mV. The different redox potentials in CH_3CN reflect different affinities of the Ni(II) derivatives for CH_3CN. Chemical reduction was accomplished by stirring THF−CH_3CN (10:1) solutions of [Ni(tmc)](OTf)$_2$ over 0.3% Na/Hg for 30 min. Filtration through Celite yielded a blue solution from which [Ni(tmc)](OTf) was precipitated in greater than 90% yield by addition of Et_2O and hexanes. UV−visible spectroscopic data were consistent with values reported in the literature,[11b,c] while

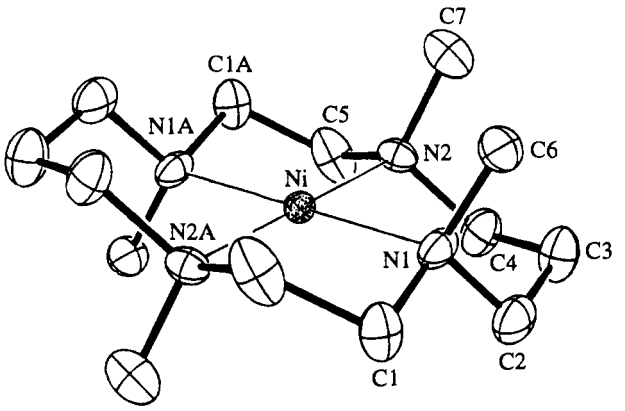

Figure 2. ORTEP of *RRSS*-[Ni(tmc)](OTf)·Na(OTf) displaying the Ni(tmc) cation only. Thermal ellipsoids are drawn at the 50% probability level. Hydrogen atoms are omitted for clarity.

analytical data agreed with the formula [Ni(tmc)](OTf)·NaOTf. This stoichiometry was confirmed by a single-crystal X-ray diffraction study. In the solid state and in the absence of O_2, [Ni(tmc)](OTf) is stable for several months.

The isomeric integrity of the Ni derivatives is not maintained upon reduction. Chemical reduction of either Ni(II) isomer resulted in production of both the *RSRS* and *RRSS*-Ni(I) isomers. Isomerization following chemical reduction of $Ni(tmc)^{2+}$ was first discussed by Espenson.[11a] Upon initial reduction, the product ratio, measured by cyclic voltammetry in CH_3CN, favored the starting Ni(II) isomer by 80%:20%.

Organic Sulfide Binding to [Ni(tmc)](OTf). [Ni(tmc)](OTf) showed no evidence of reacting with thioethers including MeCoM nor thiolates in organic solvents. Our results are consistent with the strong preference of Ni(I) for square planar coordination. This has been confirmed by structural determination of [Ni(tmc)](OTf). However, Meyerstein has reported methane production (10%) from MeCoM and similar Ni(I) macrocycles, $Ni(Me_{10}[14]aneN_4)^+$ and $Ni(tc2)^+$, in aqueous media.[6h]

Molecular Structure of *RRSS*-[Ni(tmc)](OTf)•Na(OTf). Crystals of *RRSS*-[Ni(tmc)](OTf) suitable for X-ray analysis were grown by vapor diffusion of Et_2O into saturated THF solutions. Despite the presence of both the *RSRS* and *RRSS* isomers in solution, the latter crystallized selectively presumably due to its lower solubility in THF–Et_2O. *RRSS*-[Ni(tmc)](OTf) cocrystallized with one equivalent of Na(OTf). The crystal structure consists of discrete ions with no close contacts between the $Ni(tmc)^+$ and OTf^-. A view of the cation is shown in Figure 2. Selected bond lengths and angles are contained in Table 3. The Ni ion is located on a crystallographic inversion center which relates opposite halves of the macrocycle. The coordination environment is rigorously planar (sum of the ∠N–Ni–N equals 360.0°) with two distinct Ni–N distances, 2.120(5) and 2.095(5) Å. The ligand resides in the *RRSS* configuration with unexceptional metric parameters. Two experimentally different Ni–N bond distances in square planar Ni(I) and Ni(II) complexes is becoming an increasingly common phenomena.[18] In fact, EXAFS experiments on Ni(I)–F_{430M} revealed two distinct Ni–N distances of 1.88(3) and 2.03(3) Å.[19] In the present case, the average Ni–N distance increased by 0.12 Å upon reduction from $[Ni(tmc)]^{2+}$ to $[Ni(tmc)]^+$ to accommodate the larger Ni(I) ion. Similar macrocycle core expansions of 0.11 Å for *C-R,S,S,R*-Ni(htim)$^{2+/+}$ and 0.13 Å for Ni(diene)$^{2+/+}$ have been observed.[18,20] However, for more constrained ligands, Ni(tc1)$^{2+/+}$ and Ni(tc2)$^{2+/+}$, the core size remained unchanged upon reduction.[21] Clearly, the tmc ligand is sufficiently flexible to accommodate a range of metal ion sizes or specifically, in the present case, Ni(II) and Ni(I) ions.

Table 3. Selected Bond Distances (Å) and Angles (deg)

	RRSS-[Ni(tmc)](OTf)·Na(OTf)		
Ni–N(1)	2.120(5)	Ni–N(1A)	2.120(5)
Ni–N(2)	2.095(5)	Ni–N(2A)	2.095(5)
N(1)–Ni–N(2)	93.8(2)	N(1)–Ni–N(2A)	86.2(2)
N(1)–Ni–N(1A)	180.0(1)	N(2)–Ni–N(2A)	180.0(1)
N(2)–Ni–N(1A)	86.2(2)	N(1A)–Ni–N(2A)	93.8(2)
	RRSS-Ni(tmc)SC_6H_5](OTf)		
Ni–S(1)	2.369(2)	Ni–N(3)	2.080(6)
Ni–N(1)	2.157(6)	Ni–N(4)	2.115(8)
Ni–N(2)	2.162(8)	S(1)–C(20)	1.755(8)
Ni–S(1)–C(20)	120.3(2)	N(1)–Ni–N(3)	159.5(2)
S(1)–Ni–N(1)	93.6(1)	N(1)–Ni–N(4)	84.0(3)
S(1)–Ni–N(2)	100.7(2)	N(2)–Ni–N(3)	85.0(3)
S(1)–Ni–N(3)	106.9(2)	N(2)–Ni–N(4)	160.8(2)
S(1)–Ni–N(4)	98.4(2)	N(3)–Ni–N(4)	91.1(3)
N(1)–Ni–N(2)	93.1(3)		
	RSRS-[Ni(tmc)SC_6H_5](PF$_6$)		
Ni–S(1)	2.347(2)	Ni–N(3)	2.159(7)
Ni–N(1)	2.168(7)	Ni–N(4)	2.141(5)
Ni–N(2)	2.129(6)	S(1)–C(26)	1.769(6)
Ni–S(1)–C(26)	115.2(2)	N(1)–Ni–N(3)	162.9(2)
S(1)–Ni–N(1)	99.8(2)	N(1)–Ni–N(4)	91.3(2)
S(1)–Ni–N(2)	113.2(2)	N(2)–Ni–N(3)	92.3(2)
S(1)–Ni–N(3)	97.1(1)	N(2)–Ni–N(4)	147.8(2)
S(1)–Ni–N(4)	99.0(1)	N(3)–Ni–N(4)	83.3(2)
N(1)–Ni–N(2)	83.7(3)		

Scheme 1

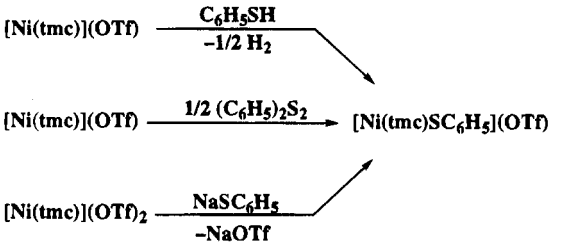

Synthesis of [Ni(tmc)SC_6H_5](OTf). Five-coordinate [Ni(tmc)SC_6H_5](OTf), may be prepared by a variety of routes, Scheme 1. Oxidative addition of C_6H_5SH or $(C_6H_5)_2S_2$ to [Ni(tmc)](OTf) yielded [Ni(tmc)SC_6H_5](OTf). In the former, the thiol protons were liberated as H_2. The disulfide reaction is discussed in detail below. Each of these reactions resulted in mixtures of *RSRS*- and *RRSS*-[Ni(tmc)SC_6H_5](OTf) as a consequence of equilibration between the isomers in the starting Ni(I) species. Consequently, procedures commencing with Ni(II) precursors are desirable to ensure isomeric integrity of the Ni product. In a typical reaction, one equivalent of $NaSC_6H_5$ was added to $[Ni(tmc)](OTf)_2$ in THF under an Ar atmosphere. An immediate change from a suspension of the complex to an intense orange solution accompanied the reaction. [Ni(tmc)-SC_6H_5](OTf) was isolated by addition of Et_2O and hexanes. In

(18) Szalda, D. J.; Fujita, E.; Sanzenbacher, R.; Paulus, H.; Elias, H. *Inorg. Chem.* **1994**, *33*, 5855–5863.

(19) (a) EXAFS of F_{430M}: Furenlid, L. R.; Renner, M. W.; Fajer, J. *J. Am. Chem. Soc.* **1990**, *112*, 8987–8989. (b) EXAFS of F_{430}: Shiemke, A. K.; Kaplan, W. A.; Hamilton, C. L.; Shelnutt, J. A. *J. Biol. Chem.* **1989**, *264*, 7276–7284.

(20) (a) Furenlid, L. R.; Renner, M. W.; Szalda, D. J.; Fujita, E. *J. Am. Chem. Soc.* **1991**, *113*, 883–892. (b) Szalda, D. J.; Fujita, E. *Acta Crystallogr.* **1992**, *C48*, 1767–1771.

(21) (a) Suh, M. P.; Shin, W.; Kim, H.; Koo, C. H. *Inorg. Chem.* **1987**, *26*, 1846–1852. (b) Suh, M. P.; Kang, S.; Goedken, V. L.; Park, S. *Inorg. Chem.* **1991**, *30*, 360–365. (c) Suh, M. P.; Kim, H. K.; Kim, M. J.; Oh, K. Y. *Inorg. Chem.* **1991**, *30*, 3620–3625.

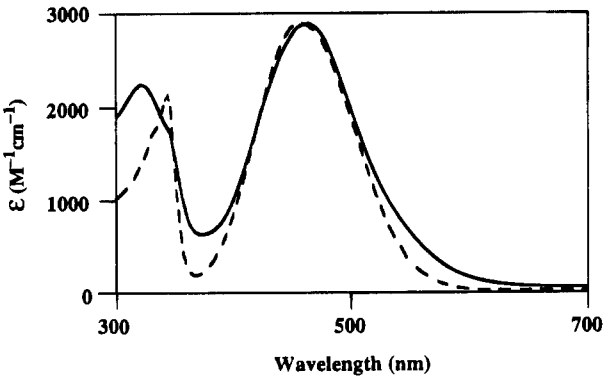

Figure 3. Electronic spectra (THF) of *RRSS*-[Ni(tmc)SC_6H_5](OTf) (− −) and (b) *RSRS*-[Ni(tmc)SC_6H_5](PF_6) (−).

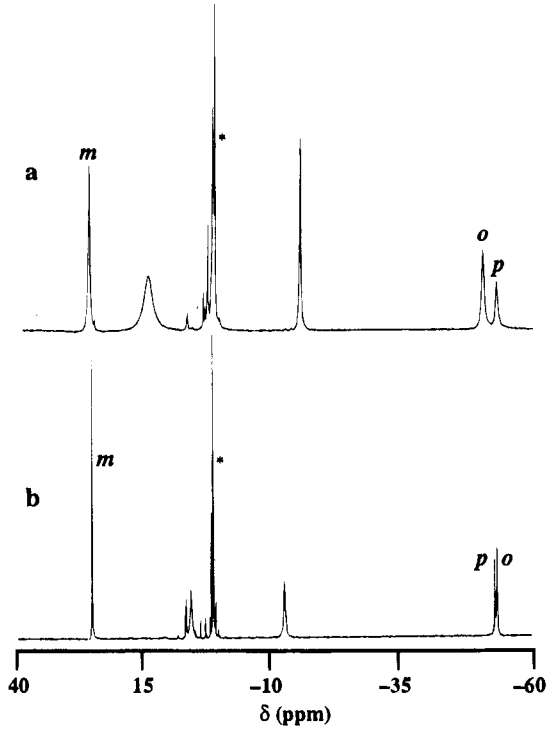

Figure 4. ^{1}H NMR spectra (acetone-d_6 = *) of (a) *RRSS*-[Ni(tmc)-SC_6H_5](OTf) and (b) *RSRS*-[Ni(tmc)SC_6H_5](PF_6).

the solid state [Ni(tmc)SC_6H_5](OTf) is stable to O_2 and moisture for several hours. In solution, [Ni(tmc)SC_6H_5](OTf) exhibits diminished stability to these antagonists. The electronic spectrum of each isomer is dominated by a ligand-to-metal charge transfer band at approximately 470 nm (Figure 3). The complexes exhibit diagnostic ^{1}H NMR spectra which show contact shifts consistent with their high spin state ($S = 1$), Figure 4. The aryl proton resonances are well removed from the diamagnetic region of the spectrum. The *ortho* and *para* protons resonate at high field, −50 ppm, while the *meta* protons are considerably deshielded, 20 ppm. The signs of the contact shifts are consistent with π spin delocalization through the aromatic substituent. For example, shifts of similar sign and magnitude are observed for the aryl ligand protons in Fe(OEP)C_6H_5 ($S = {}^1/_2$).[22] In the porphyrin complexes the *ortho* (−80 ppm) and *para* (−25 ppm) protons are highly shielded while the *meta* (20 ppm) are deshielded.

Reactions of [Ni(tmc)](OTf) with R_2S_2. Addition of R_2S_2 (R = C_6H_5, C_2H_5) to [Ni(tmc)](OTf) in THF yielded [Ni(tmc)-SR](OTf) as the only Ni-containing product. Electronic spectral changes accompanying the reaction (R = C_2H_5) are depicted in Figure 5. The production of [Ni(tmc)SC_2H_5](OTf) exhibited first-order kinetics over at least 3 half-lives under pseudo-first-order conditions, [$(C_2H_5)_2S_2$] > 10[Ni(tmc)(OTf)], as monitored by UV−visible spectroscopic changes at 414 nm. The reaction obeyed a second-order rate law: first order in each reagent. From a linear plot of k_{obs} vs [$(C_2H_5)_2S_2$], the second-order rate constant, k_1, was determined, Table 4. Oxidative addition of $(C_6H_5)_2S_2$ (k_1 = 120 M^{-1} s^{-1}) to [Ni(tmc)](OTf) is notably more facile than $(C_2H_5)_2S_2$ (k_1 = 1.9 × 10^{-3} M^{-1} s^{-1}). This significantly faster reaction could not be followed by conventional spectrophotometry. The rates were approximated by variable sweep rate cyclic voltammetry as described in the Experimental Section. The relative rates reflect differences in the S−S bond dissociation energies ($C_6H_5S-SC_6H_5$, 55 kcal mol^{-1}; $C_2H_5S-SC_2H_5$, 74 kcal mol^{-1}).[23] Products and the kinetic behavior are consistent with the mechanism contained in Scheme 2. The first step entails Ni−SR bond formation and thiyl radical production. We view this as proceeding via inner sphere electron transfer from Ni(I) to R_2S_2. In the fast second step, the thiyl radical is trapped by a second [Ni(tmc)](OTf) to yield product. Precedent for the latter reaction exists. Transition metal capture of thiyl radicals in aqueous media occurs at rates near the diffusion limit. For example, Espenson has measured rate constants for $C_2H_5S^\bullet$ reacting with $Cr(H_2O)_6(ClO_4)_2$ (4.9 × 10^8 M^{-1} s^{-1}) and Ni([14]aneN$_4$)$(ClO_4)_2$ (< 3 × 10^6 M^{-1} s^{-1}).[24] Similarly, [Ni(tmc)](OTf) has been demonstrated to efficiently capture carbon-centered radicals.[9a,11a,b]

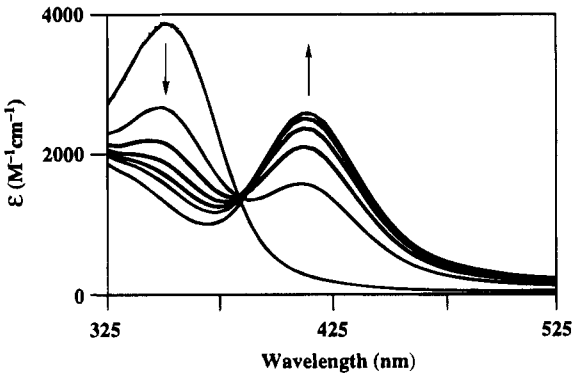

Figure 5. UV−visible spectral changes (THF) accompanying the addition of $(C_2H_5)_2S_2$ (0.36 M) to *RSRS*-[Ni(tmc)](OTf) (1.0 mM). Spectra were recorded every 30 min.

Table 4. Second-Order Rate Constants for Addition of R_2S_2 to [Ni(tmc)](OTf) in THF at 25 °C

R_2S_2	k_1, M^{-1} s^{-1}
$(C_6H_5)_2S_2$	120
$(C_2H_5)_2S_2$	1.9 × 10^{-3}

Scheme 2

$$[Ni(tmc)](OTf) + R_2S_2 \xrightarrow{k_1} [Ni(tmc)SR](OTf) + RS^\bullet$$

$$[Ni(tmc)](OTf) + RS^\bullet \xrightarrow{fast} [Ni(tmc)SR](OTf)$$

$$2\,[Ni(tmc)](OTf) + R_2S_2 \longrightarrow 2\,[Ni(tmc)SR](OTf)$$

Molecular Structures of *RSRS*-[Ni(tmc)SC_6H_5](OTf) and *RRSS*-[Ni(tmc)SC_6H_5](PF_6). The molecular structure of each isomer consists of discrete ions. A view of the cations is shown in Figure 6. Selected bond lengths and angles are contained in

(22) (a) Cocolios, P.; LaGrange, G.; Guilard, R. *J. Organomet. Chem.* **1983**, *253*, 65−79. (b) Balch, A. L.; Renner, M. W. *Inorg. Chem.* **1986**, *25*, 303−307.

(23) Benson, S. W. *Chem. Rev.* **1978**, *78*, 23−35.

(24) Huston, P.; Espenson, J. H.; Bakac, A. *J. Am. Chem. Soc.* **1992**, *114*, 9510−9516.

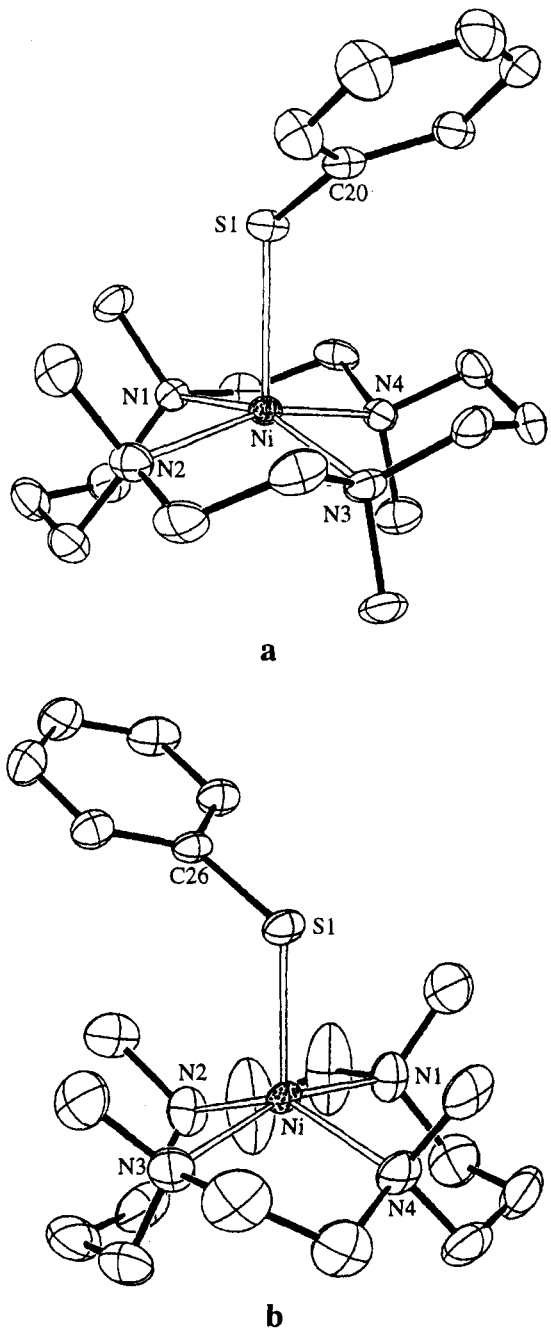

Figure 6. ORTEPs of (a) *RRSS*-[Ni(tmc)SC_6H_5](OTf) and (b) *RSRS*-[Ni(tmc)SC_6H_5](PF_6) displaying the cations only. Thermal ellipsoids are drawn at the 50% probability level. Hydrogen atoms are omitted for clarity.

Table 3. This study represents the first in which five-coordinate derivatives of each isomer have been structurally characterized and provides the unique opportunity to evaluate metrical differences between the two isomers. The geometry about the Ni ion in *RRSS*-[Ni(tmc)SC_6H_5](OTf) is close to an idealized square pyramid. The four amine nitrogens provide basal ligation with Ni–N distances averaging 2.128(14) Å and the sulfur occupies the apical position, Ni–S, 2.369(2) Å. The S–Ni–N angles range from 93.6 to 106.9°. The ∠Ni–S–C(20) of 120.3-(2)° is comparable to that of other metal thiolates.[25] The C_6H_5 substituent resides directly above N(3) as evidenced by the

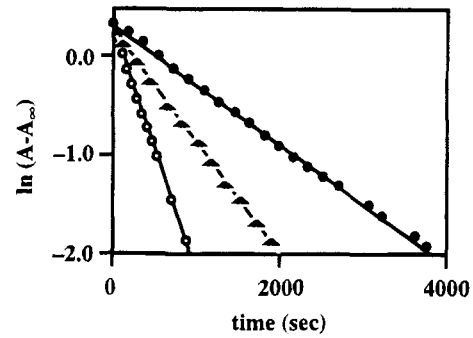

Figure 7. Pseudo-first-order plots of the alkylation of *RRSS*-[Ni(tmc)-SC_6H_5](OTf) (0.50–1.0 mM) with CH_3I (●, 7.0 mM; ▲, 13 mM; ○, 28 mM) in THF–CH_3CN (1:1) at 25 °C.

N(3)–Ni–S–C(20) dihedral angle of 1.20°. Since the CH_3 group on N(3) points away from the thiolate ligand, the orientation of the aryl minimizes steric repulsions between it and the macrocycle. The gross structural features of *RSRS*-[Ni(tmc)SC_6H_5](PF_6) are similar to *RRSS*-[Ni(tmc)SC_6H_5](OTf). As with every other crystallographically characterized derivative,[26] the axial ligand is located on the same face of the tmc as the four amine CH_3 substituents. The average Ni–N distances (2.149(13) Å) of *RSRS*-[Ni(tmc)SC_6H_5](PF_6) are longer than for the *RRSS* isomer by 0.021 Å. These are somewhat offset by a shorter Ni–S bond, 2.352(2) Å. The ∠Ni–S–C(26) is more acute by 5.1°. This is surprising because the repulsive steric interactions between the thiolate and tmc appear more demonstrative in this isomer. One of the amine nitrogens, N(2), which is nearly eclipsed by the S–C vector (dihedral angle equals 5.1°), is markedly displaced below the least-squares plane defined by the remaining N atoms, resulting in a distorted square pyramidal coordination sphere. The movement of N(2) may be rationalized as abating repulsive interactions between the C_6H_5 substituent and the CH_3 group on N(2). The closest contact is 3.36 Å (C(12)--C(26)). The average Ni–N distances are comparable with those in other structurally characterized Ni(tmc)X^+ complexes and are in accord with the high spin state.[26] For example, in *RSRS*-[Ni(tmc)N_3](ClO_4), Ni–N_{av} equals 2.103 Å,[26b] and in *RSRS*-[Ni(tmc)($NCCH_3$)](ClO_4)$_2$, Ni–N_{av} equals 2.143 Å.[26d] The differences in ground state structures of the two isomers, particularly the nickel–ligand bond distances, are manifest in the relative rates of reaction with haloalkanes.

Alkylation of [Ni(tmc)SC_6H_5](OTf). Reaction of [Ni(tmc)-SC_6H_5](OTf) with haloalkane in THF-CH_3CN (1:1) results in quantitative formation of the products indicated in eq 2. The

$$[Ni(tmc)SC_6H_5](OTf) + RX \xrightarrow{k_2} [Ni(tmc)X](OTf) + RSC_6H_5 \quad (2)$$

rates of reaction were monitored by UV–visible spectral changes which exhibited isosbestic behavior. Under pseudo-first-order conditions, [RX] > 20 [Ni(tmc)SC_6H_5(OTf)], the alkylation exhibited first-order kinetics over at least three half-lives, Figure 7. The reaction obeyed a second-order rate law: first order in each reagent, Table 5. Second-order rate constants are listed in Table 6. The trend of rate constants for RI, R =

(25) (a) Liaw, W.-F.; Kim, C.; Darensbourg, M. Y.; Rheingold, A. L. *J. Am. Chem. Soc.* **1989**, *111*, 3591–3592. (b) Darensbourg, M. Y.; Longridge, E. M.; Payne, V.; Riordan, C. G.; Springs, J. J.; Reibenspies, J.; Calabrese, J. *Inorg. Chem.* **1990**, *29*, 2721–2726.

(26) (a) Wagner, F.; Mocella, M. T.; D'Aniello, M. J.; Wang, A. H.-J.; Barefield E.K. *J. Am. Chem. Soc.* **1974**, *96*, 2625–2627. (b) D'Aniello, M. J.; Mocella, M. T.; Wagner, F.; Barefield, E. K.; Paul I. C. *J. Am. Chem. Soc.* **1975**, *97*, 192–194. (c) Lincoln, S. F.; Hambley, T. W.; Pisaniello, D. L.; Coates, J. H. *Aust. J. Chem.* **1984**, *37*, 713–723. (d) Crick, I. S.; Hoskins, B. F.; Tregloan, P. A. *Inorg. Chim. Acta* **1986**, *114*, L33–L34.

Table 5. Dependence of k_{obs} on [RX] for Reaction of [Ni(tmc)SC_6H_5](OTf) with RX in THF−CH_3CN (1:1) at 25 °C

RX	[RX], M	10^3k_{obs}, s^{-1}
	RRSS-[Ni(tmc)SC_6H_5](OTf)	
C_2H_5I	0.0083	1.1
	0.016	1.9
	0.044	7.3
	0.12	21
	0.28	33
$(CH_3)_2CHI$[a]	0.22	0.65
	0.45	0.84
	0.65	1.6
	1.0	1.9
	1.3	2.1
	1.9	2.4
$C_6H_5CH_2Cl$	0.014	2.1
	0.029	3.5
	0.058	7.6
	0.10	12
	0.16	21
	0.22	25
	RSRS-[Ni(tmc)SC_6H_5](OTf)	
CH_3I	0.066	1.2
	0.17	3.0
	0.25	3.1
	0.35	5.3
	0.78	9.1
	1.17	14
C_2H_5I	0.24	0.11
	0.47	0.18
	0.87	0.43
	1.4	0.67
	1.9	0.72

[a] Measured in 100% CH_3CN.

Table 6. Second-Order Rate Constants for Alkylation of [Ni(tmc)SPh](OTf) in THF−CH_3CN (1:1) at 25 °C

	k_2, M^{-1} s^{-1}	
RX	*RSRS*-[Ni(tmc)SC_6H_5](OTf)	*RRSS*-[Ni(tmc)SC_6H_5](OTf)
CH_3I	1.2×10^{-2}	4.1
C_2H_5I	4.0×10^{-4}	0.14
$(CH_3)_2CHI$	$\approx 7.1 \times 10^{-6}$	1.1×10^{-3}
$C_6H_5CH_2Cl$		0.12

$CH_3 > C_2H_5 > (CH_3)_2CH$, is consistent with S_N2 alkylation of the thiolate. Alkylation of metal thiolates may lead to isolable metal-bound thioethers.[25,27] However, in the present case the thioether is a weaker ligand than I^- and does not effectively compete for the available coordination site. Significantly, the rates of alkylation of the two Ni isomers exhibit large differences. For a given RX, *ca.* $k_2^{RRSS}/k_2^{RSRS} = 350$. Taken together, the rate law, the rate dependence on RX and the rate differences between the isomers are consistent with alkylation at Ni-bound thiolate. Were alkylation to occur at unbound thiolate, mixed second-order kinetics would be expected and the rates would be independent of isomer. S_N2 alkylation of metal-bound thiolates has been demonstrated by several groups.[25,27] A thorough kinetic study of the alkylation of $CpFe(CO)_2SR$ yielding $CpFe(CO)_2(RSR')$ supported a nucleophilic substitiution pathway.[27] The effect of haloalkane ($CH_3I > C_2H_5I >> (CH_3)_2CHI = (CH_3)_3CI = 0$) and solvent polarity ($Me_2SO >$ acetone) on the reaction rate were most consistent with such substitution. While the limited stability of [Ni(tmc)SC_6H_5](OTf) in a range of solvents precluded solvent polarity studies, the effect of haloalkane on reaction rates paralleled that measured for $CpFe(CO)_2SR$. The rate differences between the isomers is in accord with the relative ground state structures determined crystallographically.[28] *RRSS*-[Ni(tmc)SC_6H_5](OTf) possesses a longer Ni−S bond distance and shorter Ni−N bonds than the *RSRS* isomer. This is consistent with *weaker* Ni−SC_6H_5 bonding and consequently, a less distorted Ni coordination sphere relative to the four-coordinate complex. The (thermodynamically) weaker thiolate ligation results in a more kinetically accessible alkylation at the sulfur lone pair. Conversely, the structural variances of *RSRS*-[Ni(tmc)SC_6H_5](PF_6), a shorter Ni−S bond distance and more distorted macrocycle core, point to a more stable, less reactive Ni−SC_6H_5 moiety. Qualitative differences in reaction rates of the two Ni isomers have been documented previously. Reactions of haloalkanes with organonickel complexes, [Ni(tmc)R](ClO_4), showed a similar dependence on isomer identity.[11b,c] *RRSS*-[Ni(tmc)R](ClO_4) reacted significantly faster than *RSRS*-[Ni(tmc)R](ClO_4).

In addition to a clean S_N2 pathway, deviations from second-order kinetics were observed for slower reactions ($(CH_3)_2CHI$ and $C_6H_5CH_2Cl$ reacting with the *RSRS* isomer). These data could be fit with a three term rate law which took into account Ni−SC_6H_5 bond dissociation and fast alkylation of the free $SC_6H_5^-$ (see Experimental Section).[29]

Summary

The following are the principal findings and conclusions of this study.

(1) [Ni(tmc)]$(OTf)_2$ binds organic sulfides weakly to form high spin, five-coordinate species. $(CH_3)_2S$ and $(C_2H_5)_2S$ coordinate to the *RSRS* and *RRSS* isomers with equal affinities, while aryl-substituted sulfides, $C_6H_5SCH_3$, do not coordinate. The donor ability of the sulfides falls below that of common solvents: H_2O, Me_2SO, and CH_3CN.

(2) [Ni(tmc)]$(OTf)_2$ binds MeCoM strongly in organic media: coordination, dictated by electrostatics, is via the sulfonate rather than the thioether.

(3) The Ni(I) complex, *RRSS*-[Ni(tmc)](OTf), has been crystallographically characterized. The Ni ion coordination sphere is rigorously planar with two sets of distinct Ni−N bond distances: 2.120(5) and 2.095(5) Å. The macrocycle core expansion is in accord with Ni-centered reduction.

(4) *RSRS*-[Ni(tmc)SC_6H_5](OTf) and *RRSS*-[Ni(tmc)SC_6H_5](OTf) may be synthesized by a variety of routes. However, to insure isomeric purity, the corresponding [Ni(tmc)]$(OTf)_2$ must be employed as starting material.

(5) Consistent with structural differences in the solid state, *RRSS*-[Ni(tmc)SC_6H_5](OTf) reacts with haloalkanes 350 times more rapidly than *RSRS*-[Ni(tmc)SC_6H_5](OTf). Alkylation occurs at Ni-bound thiolate and not via a dissociative pathway involving Ni−SC_6H_5 bond cleavage.

(27) Ashby, M. T.; Enemark, J. H.; Lichtenberger, D. L. *Inorg. Chem.* **1988**, *27*, 191−197.

(28) A reviewer has suggested the kinetic differences we observe here result from differences in accessibility of the sulfur to the electrophile, i.e., steric effects due to the presence of four methyl groups surrounding the sulfur in the *RSRS* diastereomer, whereas there are only two in the *RRSS* diastereomer. Clearly, this can not be the case as the *RSRS* isomer is more accessible on the side containing the four methyl groups. This contention is evidenced by the structures of five-coordinate derivatives of the *RSRS* isomer which **always** show the fifth ligand bound to the same side as the methyl groups. In other words, the ethylene and propylene linkers of tmc are more sterically demanding than the methyl groups. Furthermore, the kinetic and structural *trans* effects of alkyl groups have been well documented in organocobalt chemistry. (a) Stewart, R. C.; Marzilli, L. G. *J. Am. Chem. Soc.* **1978**, *100*, 817. (b) Bakac, A.; Espenson, J. H. *J. Am. Chem. Soc.* **1984**, *106*, 5197−5202.

(29) At high [I^-] (added [Bu_4N]I), an I^--catalyzed pathway which becomes significant. In the presence of 30 equiv of I^-, there are no UV−visible spectral changes observed for [Ni(tmc)SC_6H_5](OTf).

Our results suggest that the [Ni(tmc)](OTf) system is ideally suited to explore the role of the HS−HTP cofactor in promoting F_{430} catalysis. In this regard, we are currently exploiting the reaction of R_2S_2 with [Ni(tmc)](OTf) in the presence of MeCoM to evaluate the ability of thiyl radicals to activate MeCoM towards C−S bond rupture.[30]

Acknowledgment. We gratefully acknowledge the financial support of the NSF (Grant OSR-9255223), the Exxon Educational Fund and the donors of the Petroleum Research Fund, administered by the American Chemical Society (Grant 27076-G3). C.G.R. thanks the NSF for a National Young Investigator Award (1994−1999). Garry Williams and Timothy Hubin are thanked for their assistance in the synthesis of [Ni(tmc)SC_6H_5](OTf) and [Ni(tmc)](OTf), respectively. We thank the reviewers for their helpful comments.

Supporting Information Available: Tables giving structure determination summary, atomic coordinates, complete bond lengths and bond angles, anisotropic thermal parameters, and hydrogen atom parameters for *RRSS*-[Ni(tmc)](OTf), *RSRS*-[Ni(tmc)SC_6H_5](PF_6), and *RRSS*-[Ni(tmc)SC_6H_5](OTf) (27 pages). Ordering information is given on any current masthead page.

IC950699N

(30) Berkessel, A. *Bioorganic Chem.* **1991**, *19*, 101−115.